Journal of Molecular Neuroscience (2024) 74:98
https://doi.org/10.1007/s12031-024-02276-6

RESEARCH

Effects of Electroacupuncture at Varied Frequencies on Analgesia and Mechanisms in Sciatic Nerve Cuffing-Induced Neuropathic Pain Mice

Kexin Fang[1,2] · **Wen Cheng**[1,2] · **Bin Yu**[1,2]

Received: 19 August 2024 / Accepted: 3 October 2024

Abstract

Addressing the intricate challenge of chronic neuropathic pain has significant implications for the physical and psychological well-being of patients, given its enduring nature. In contrast to opioids, electroacupuncture (EA) may potentially provide a safer and more efficacious therapeutic alternative. Our objective is to investigate the distinct analgesic effects and potential mechanisms of EA at frequencies of 2 Hz, 100 Hz, and 18 kHz in order to establish more precise frequency selection criteria for clinical interventions. Analgesic efficacy was evaluated through the measurement of mice's mechanical and thermal pain thresholds. Spinal cord inflammatory cytokines and neuropeptides were quantified via Quantitative Real-time PCR (qRT-PCR), Western blot, and immunofluorescence. Additionally, RNA sequencing (RNA-Seq) was conducted on the spinal cord from mice in the 18 kHz EA group for comprehensive transcriptomic analysis. The analgesic effect of EA on neuropathic pain in mice was frequency-dependent. Stimulation at 18 kHz provided superior and prolonged relief compared to 2 Hz and 100 Hz. Our research suggests that EA at frequencies of 2 Hz, 100 Hz, and 18 kHz significantly reduce the release of inflammatory cytokines. The analgesic effects of 2 Hz and 100 Hz stimulation are due to frequency-dependent regulation of opioid release in the spinal cord. Furthermore, 18 kHz stimulation has been shown to reduce spinal neuronal excitability by modulating the serotonergic pathway and downstream receptors in the spinal cord to alleviate neuropathic pain.

Keywords Electroacupuncture · Neuropathic pain · Opioid peptides · Spinal cord · Serotonergic pathway

Introduction

Neuropathic pain, caused by damage or disease affecting the somatosensory nervous system, is a common occurrence in the general populace, with rates reaching up to 8%. Notably, its occurrence is even more pronounced among specific subgroups, including individuals with diabetes, acquired Immune Deficiency Syndrome (AIDS), and cancer (Gilron et al. 2015). This persistent pain not only exacerbates depression and anxiety in patients but also leads to sleep disturbances, significantly impacting their daily activities and quality of life (Attal et al. 2010). Current pharmacological treatments for neuropathic pain, include ion channel drugs and tricyclic antidepressants; however, their long treatment periods, severe side effects, and unclear efficacy limit their long-term clinical applications. Additionally, for certain patients suffering from neuropathic radicular pain, while surgical decompression may relieve the associated symptoms, the incidence of persistent and refractory post-laminectomy syndrome or failed back surgery syndrome still ranges between 10% and 40% (Dworkin et al. 2013). Therefore, the search for innovative treatments that can provide long-term relief from neuropathic pain, especially alternatives to pharmacological interventions, is of paramount clinical significance (Varga et al. 2023).

EA, as a non-pharmacological modality, is being extensively utilized in the realm of pain management. EA boast distinct advantages such as rapid onset of action, minimal invasiveness, selectivity, and precision in control (Knotkova et al. 2021; Xu et al. 2003). The efficacy of EA in alleviating discomfort is influenced by several crucial factors, including

✉ Bin Yu
yubin@tongji.edu.cn

[1] Tongji University School of Medicine, Shanghai, China

[2] Department of Anesthesiology, Yangzhi Rehabilitation Hospital Affiliated to Tongji University, School of Medicine, Tongji University, 2209 Guangxing Road, Songjiang District, Shanghai, China

Published online: 17 October 2024

duration, frequency, intensity, and characteristics of the output waveform (Fan et al. 2023; Jiang et al. 2022). Previous studies have shown that stimulation at frequencies between 1 and 1000 Hz activates myelinated fibers, releasing inhibitory neurotransmitters (Thuvarakan et al. 2020), thereby mitigating conditions such as bone cancer-induced pain or abnormal sensations due to neural impairment (Chen et al. 2015; Jiang et al. 2021; Oberoi et al. 2022). In clinical practice, 20 Hz stimulation is preferred for chronic cases, while 100 Hz stimulation is used for managing acute discomfort. Alternating 20 Hz/100Hz stimulation during surgical procedures not only ensures intraoperative comfort but also reduces opioid consumption and provides postoperative relief. Moreover, EA within the 1-to-100 kHz spectrum, known as kilohertz high frequency electroacupuncture stimulation (KHES), effectively attenuates neuropathic discomfort by blocking nerve conduction, for instance, a 10–20 kHz blockage can safely relieve distress from neurofibroma-related amputation for several hours (Soin et al. 2015). Similarly, a 10 kHz blockage at the thoracic level significantly diminishes backache without causing noticeable sensory aberrations (Miller et al. 2016; Tiede et al. 2013).

Several studies have revealed that the pain-relief mechanism of EA functions distinctively across varying frequencies. Both 2 Hz and 100 Hz frequencies can ameliorate neuropathic pain by modulating the release of different central nervous system peptides (Chen and Han 1992; Wang et al. 1990). At the spinal level, 2 Hz EA can induce the release of enkephalin and endorphin (Cuitavi et al. 2021; Lee et al. 2009), Conversely, 100 Hz EA can augment the release of dynorphin, thus mitigating hyperalgesia responses induced by neuropathic pain (Wu et al. 1999; Zhou et al. 2015). A growing body of research has revealed that both 2 Hz and 100 Hz frequencies exhibit regulatory effects on inflammatory cytokines within the spinal cord. Notably, studies have indicated that 2 Hz EA significantly inhibits the activation of pain-related cytokines in the spinal cords of complete freund's adjuvant(CFA)-induced mice, including interleukin-1 beta(IL-1β), interleukin-6(IL-6) and tumor necrosis factor alpha(TNF-α) (Li et al. 2019). Furthermore, treatment with 2 Hz/100Hz EA promotes the activation of Treg cells in spinal cord, suppresses macrophages and neutrophils, reduces the expression of IL-1β, NLR Family Pyrin Domain Containing Protein 3 (NLRP3), and TNF-α, and ultimately alleviates pain in CFA mice (Yu et al. 2020). Our previous research demonstrated that neuropathic pain could result in heightened excitability and abnormal discharge of sensory neurons, stemming from the disruption of pathways that regulate the electrical excitability of nerve cells (Lu et al. 2023). However, KHES displayed potential in relieving neuropathic pain through its high-frequency electric field, which could close or inhibit ion channels. Through electromyography recordings, we determined that the optimal blocking parameter for KHES is 18 kHz at 0.5 milliamperes (Fang et al. 2024).

Several studies suggest that the analgesic effects of KHES may be associated with serotoninergic mechanisms. The neurotransmitter 5-hydroxytryptamine (5-HT) is extensively distributed across both the peripheral and central nervous systems. Upon binding to 5-HT receptors, it can modulate pain signal processing within the spinal cord, leading to either facilitatory or inhibitory effects (Lee et al. 2015). The descending serotoninergic system originates from brainstem regions, including the raphe nuclei, dorsal raphe nucleus (DRN), and ventrolateral medulla (VLM) (Heijmans et al. 2021; Schwaller et al. 2017). In contrast, the ascending serotonin system includes regions such as anterior cingulate cortex (ACC) and rostral ventrolateral medulla (RVM) (Chen et al. 2018; Mo et al. 2023; Tavares and Lima 2002). Various subtypes of 5-HT receptors are implicated in the regulation of this serotoninergic system and are integral to pain modulation due to their capacity to elicit diverse effects under painful conditions (Cortes-Altamirano et al. 2018; Haleem 2018; Sánchez-Brualla et al. 2018). Elucidating the role of these mechanisms in the context of KHES for pain relief necessitates further investigation.

The objective of this study is to examine the analgesic efficacy and underlying mechanisms of action of three different frequencies of EA in sciatic nerve cuffing-induced neuropathic pain mice (Benbouzid et al. 2008; Mosconi and Kruger 1996). The research endeavors to ascertain whether KHES, similar to conventional low-frequency EA, affects the release of neuropeptides and inflammatory cytokines in the central nervous system. If this is not the case, the study will delve into the mechanisms by which KHES alleviates neuropathic pain in sciatic nerve cuffing mice.

Materials and Methods

Experimental Animals

We acquired 50 adult male C57BL/6 mice, aged 7–8 weeks and weighing between 20 and 30 g, from Shanghai SLAC Laboratory Animal Co., Ltd. [License No. SCXK (Shanghai) 2022-0004]. The temperature and humidity of all experiments were kept stable (12-h light/dark cycle at 23 ± 2 °C, 45–55% humidity). The mice could freely obtain food and water. All experimental procedures were conducted at Tongji university in accordance with ethical standards for the use of research animals, following the relevant guidelines and regulations of the International Association for the Study of Pain.

Sciatic Nerve Cuffing-induced Neuropathic Pain Mice

We randomly assigned the mice into five groups: the sham group, the cuff group, the 2HzEA group, the 100HzEA group and the 18kHzEA group. After administering

anesthesia with 0.8% pentobarbital sodium, careful separation of surrounding tissues allowed for exposure of the sciatic nerve. To induce chronic constriction injury, a polyethylene tube was tied around the sciatic nerve. Successful confirmation of ligation involved observing slight muscle twitching upon gentle pressure on the tube (Benbouzid et al. 2008; Mosconi and Kruger 1996; Pitcher et al. 1999). In the sham group, cuff modeling procedure was performed without manipulation of the sciatic nerve itself.

Experimental Procedure for EA

The mice were securely positioned on a platform in a right lateral position after inducing anesthesia with 2% isoflurane. The fur of the mice was carefully shaved off and the puncture site was disinfected with alcohol. Zusanli (ST36) was selected as the EA stimulation point, situated approximately 2 mm beneath the small fibula head on the lateral side of the hind limb knee joint. Stainless-steel needles with a diameter of 0.3 mm and a length of 13 mm were inserted into ST-36 at a depth of 2 to 3 mm. The stimulation frequency provided by the NeuroMax neurophysiological stimulator (NuoCheng Co., Ltd., China) was adjusted to 2 Hz, 100 Hz, and 18 kHz from the 7th to the 13th day after modeling. Current intensity rang was 0.5 mA (Fang et al. 2024). The time control consisted of a 10-second stimulation time followed by a 5-second rest, with the total time reaching 30 min, and the stimulus waveform was a biphasic rectangular wave. The stimulation pulse width was calculated according to formula: pulse width $=[(1/\text{frequency}) \times 0.8]/2 \times 106$, the occupation ratio was 0.8 (Ling et al. 2019). In the sham surgery group, electrodes were inserted using similar methods but without concurrent electrical stimulation applied.

Behavioral Studies

For all behavioral testing, the mice were exposed to the testing environment without any stimulation for 2 h per day for 3 days before the formal testing and the investigators were blinded to the treatment. Behavioral tests were performed when the mice were calm but not sleeping, and the test time was fixed at 9:00 AM–6:00 P.M. According to the experimental procedure shown in Fig. 1, the mice were tested with varying intensities (0.04, 0.07, 0.16, 0.4, 1, 1.4, and 2 g) of Von Frey fibers (Shanghai Yuyan Instrument Co., Ltd., China). The Von Frey filament was vertically stimulated on the hind paw near the palm for 5–6 s, and positive responses were recorded when the mice exhibited paw withdrawal or licking behavior. Finally, the mouse's paw withdrawal threshold (PWT) was determined using the non-parametric Dixon test method (Chaplan et al. 1994). We utilized a thermal pain stimulation device (Shanghai Yuyan Instrument Co., Ltd., China) to assess the thermal withdrawal latency (TWL). The laser stimulation was administered to the plantar area of the hind paws, about 0.5 cm from the plantar surface, with a maximum duration of 20 s. Precautions were taken to prevent tissue damage from prolonged exposure or heat generation during testing sessions. If paw withdrawal or licking behavior occurred in response to the laser application, it was immediately ceased and the time was noted. This procedure was repeated three times with at least 10 min between each stimulation (Hargreaves et al. 1988). The mean duration of the three stimulations was utilized to determine the TWL of the mice.

RNA Isolation and Quality Assessment

After the completion of behavioral studies, 13 days post sciatic nerve cuffing, total RNA was extracted from the spinal cords of mice in the sham group, cuff group, and 18 kHz group using the RNAmini kit (Qiagen, Germany). The quality of the RNA was assessed through agarose gel electrophoresis

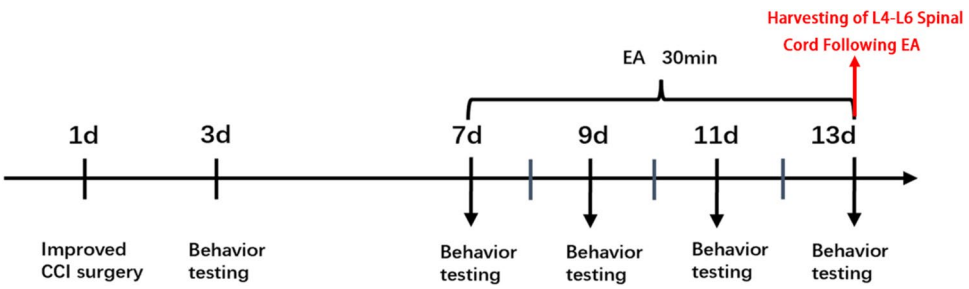

Fig. 1 Experimental design timeline. Surgical procedures were performed on Day 1, followed by the administration of EA from Day 7 to Day 13. Behavioral assessments took place on Day 3, Day 7, Day 9, Day 11, and Day 13. After a period of 13 days, the mice were humanely euthanized and their spinal cords were collected for analysis

and Qubit (Thermo Fisher Scientific, Waltham, MA, USA). RNA samples from seven to nine biological replicates at each time point (0, 12, 36, and 72 h) were pooled into three equal-sized independent pools for RNA sequencing. Subsequently, a strand-specific library was prepared using the TruSeq RNA sample preparation kit (Illumina Inc., San Diego, CA) and sequenced on an Illumina Novaseq 6000 instrument.

Differential Gene Expression Analysis

Differential gene expression analysis was performed by aligning preprocessed sequences to reference genomic sequences using STAR software, followed by statistical analysis of the alignment results with RSEQC. DESeq2 software was used for experiments involving repeated samples, while DESeq software was used experiments those without repeated samples. Genes were identified as differentially expressed if they have a p-value $<=0.05$ and exhibit at least a 2-fold difference in expression between sample groups, and the Benjamini & Hochberg multiple testing correction method was applied to obtain q-values for each gene. The False Discovery Rate (FDR) value was also calculated to assess reliability, and TopGO software was utilized for Gene Ontology (GO) function analysis on the set of target genes, while Kyoto Encyclopedia of Genes and Genomes (KEGG) pathway function analysis was performed to annotate and classify these genes based on their functions in the KEGG database.

Quantitative Reverse-transcriptase Polymerase Chain Reaction

We procured the L4-L6 spinal dorsal horn for qRT-PCR analysis and performed total RNA extraction using TRIzol. Reverse transcription was carried out using oligo-DT primers from Sangon Biotech Co., Ltd, China. Each sample underwent triplicate division, with 20 µL per replicate comprising 10 µL of forward and reverse primers, as well as 10 µL of Synergetic Binding Reagent (SYBR) Green Super Mix (Invitrogen) and 25 ng of cDNA. The reactions were conducted on the Applied Biosystems 7500 Fast Real-Time PCR System. Relative expression levels of mRNA in spinal cord tissue were determined using the 2-ΔΔCt method. The specific primers selected for qRT-PCR encompass included glyceraldehyde-3-phosphate dehydrogenase (GAPDH), proopiomelanocortin (POMC), proenkephalin (PENK), prodynorphin (PDYN), TNF-α, IL-1β, 5-hydroxytryptamine 1 A receptor (5-HT1A), 5-HT1B, 5-HT2A, 5-HT2B, 5-HT3A, 5-HT4A and 5-HT5A; as well as G protein-gated inwardly rectifying potassium channels 1(GIRK1), GIRK2, GIRK3, and GIRK4; the N-type voltage-gated calcium channel(Cav2.2); calcium/calmodulin-dependent protein kinase II (CaMKII) and N-methyl-D-aspartate receptor-2B (NMDAR2B).Mouse-specific primer sequences utilized for detection are detailed in Table 1 provided by Sangon.

Western Blotting

After the completion of behavioral studies, 13 days post sciatic nerve cuffing, mice were anesthetized using 2% isoflurane, and the lumbar spinal cord from L4 to L6 was removed. The proteins were separated through sodium dodecyl sulfate-polyacrylamide gel electrophoresis (SDS-PAGE) on gels with varying concentrations (7.5%, 10%, or 15%) and subsequently transferred onto polyvinylidene difluoride (PVDF) membranes. Following this step, the membranes underwent incubation in blocking buffer for 2 h followed by overnight exposure to primary antibodies at 4 °C, including POMC (1:2000, 66358-1-Ig, Proteintech Group, Inc.), enkephalin (1:1000, ab77273, Abcam, Inc.), dynorphin A (1:1000, ab8250, Abcam, Inc.), TNF-α(1:1500, D2D4, Cell Signaling Technology, Inc.), IL-1β(1:1500,D3U3E, Cell Signaling Technology, Inc), 5HT2A (1:1000, GB111001-50, Servicebio, Inc), 5HT2B (1:1000, 26408-1-AP, Proteintech Group, Inc.), tubulin (1:5000; HRP-66031; Proteintech Group, Inc.) and GAPDH (1:1500, D16H11, Cell Signaling Technology, Inc.). After three washes with tris-buffered saline and Tween-20(TBST), the membranes were exposed to secondary antibodies such as horseradish peroxidase (HRP)-conjugated AffiniPure goat anti-mouse IgG (1:5000, Cat. No. SA00001-1, Proteintech Group, Inc.), HRP-conjugated AffiniPure goat anti-rabbit IgG (1:5000, Cat. No. SA00001-2, Proteintech Group, Inc.) and Rabbit Anti-Goat IgG (1:5000, ab6741, Abcam, Inc.). Finally, enhanced chemiluminescence substrate was used to visualize the bands which were then analyzed for intensity using ImageJ software.

Immunofluorescence

Five groups of mice were anesthetized with 2% isoflurane before undergoing a thorough perfusion with a solution composed of 0.9% saline and 4% formalin. Subsequently, the L4-L6 spinal cord segments were meticulously excised and securely fixed in position. The spinal cord tissue was then carefully sectioned at a controlled temperature of 25 °C using a precision cryostat, followed by immunofluorescence staining to enhance visualization. Following a thorough rinse with phosphate-buffered normal saline (PBS), the sections were gently permeabilized with 0.3% Triton X-100. This was followed by a two-hour incubation in 10% normal goat serum to block non-specific binding. The primary antibody markers utilized were POMC (1:400, Proteintech Group, Mouse, 66358-1-Ig) and dynorphin A

Table 1 Sequences (5′-3′) of primers used in qRT-PCR

Gene	Forward primer	Reverse primer
GAPDH	AATGGATTTGGACGCATTGGT	TTTGCACTGGTACGTGTTGAT
POMC	CCTATCGGGTGGAGCACTTC	TGGCTCTTCTCGGAGGTCAT
PENK	ATGGCGTTCCTGAGACTTTGA	TAGAGTTTTGGCGTATTTCGGAGGC
PDYN	ACTGCCTGTCCTTGTGTTCC	CCAAAGCAACCTCATTCTCC
TNF−α	GGAACTGGCAGAAGAGGCACTCCCC	GGCCATTTGGGAACTTCTCATCCCTTT
IL−1β	CCTGTGTCTTTCCCGTGGACCTTCCAGG	CATCATCCCATGAGTCACAGAGGATGGG
5−HT1A	GACAGGCGGCAACGATACT	CCAAGGAGCCGATGAGATAGTT
5−HT1B	CGCCGACGGCTACATTTAC	TAGCTTCCGGGTCCGATACA
5−HT2A	TAATGCAATTAGGTGACGACTCG	GCAGGAGAGGTTGGTTCTGTTT
5−HT2B	GAACAAAGCACAACTTCTGAGC	CCGCGAGTATCAGGAGAGC
5−HT3A	CCTGGCTAACTACAAGAAGGGG	TGCAGAAACTCATCAGTCCAGTA
5−HT4A	AGTTCCAACGAGGGTTTCAGG	CAGCAGGTTGCCCAAGATG
5−HT5A	ATGGATCTGCCTGTAAACTTGAC	CACTCGGAAAGCTGAGAGAAAA
GIRK1	GGGGACGATTACCAGGTAGTG	CGCTGCCGTTTCTTCTTGG
GIRK2	ACCAGCCAAAGTTGCCTAAG	CTTCCTCACGTACCTCTGGAT
GIRK3	GAAGGACGGTCGCTGTAACG	CGTGGTGAACAGGTCGGTC
GIRK4	GCCGGTGATTCTAGGAATGCT	TCACTTAGGTAGCGGTAGGTTT
Cav2.2	ACAACGTCGTCCGCAAATAC	CAGGGCCAGAACAATGCAGT
CaMKII	TCCAGAAGTCCTGCGTAAAGA	CCACCAGCAAGATGTAGAGGAT
NMDAR2B	GCCATGAACGAGACTGACCC	GCTTCCTGGTCCGTGTCATC

(1:200, Abcam, Rabbit, ab8250), ensuring specific targeting of the desired proteins. To visualize the nuclei, 4,6-diamino-2-phenyl indole (DAPI) was applied at a concentration of 5 μg/ml. Alexa Fluor 350 and 488 secondary antibodies were then used to label the nuclei, with an additional two-hour incubation period to ensure optimal binding. The stained sections were finally imaged using a state-of-the-art Zeiss LSM510 confocal microscope (Zeiss, Thornwood, CA, USA), capturing high-resolution images for detailed analysis.

Statistical Analyses

The mean ± SEM was used to represent the data, and statistical analysis was carried out with SPSS 22.0 software. A one-way ANOVA was conducted, followed by a Tukey post-hoc test for comparing multiple groups. Statistical significance was considered at $p < 0.05$.

Results

Comparing the Analgesic Effects of Different Frequency EA

The cuff group exhibited significantly reduced PWT and TWL on Day 3 and Day 7 compared to the sham group, indicating successful sciatic nerve cuffing mouse modeling (Fig. 2A, $p < 0.001$; Fig. 2B, $p < 0.05$). EA at frequencies of 2 Hz, 100 Hz, and 18 kHz respectively was administered from Day 7 to Day 13 post-modeling. For each 30-minute stimulation session, the mice were maintained under general anesthesia using a 2% isoflurane gas mixture. One hour after stimulation, the PWT was reassessed to gauge the analgesic duration. The antinociceptive effect of 2 Hz EA on mechanically induced pain lasted for 1 h on Day 7 (Fig. 2C, $p < 0.05$), extended to 2 h on Day 9 (Fig. 2D, $p < 0.05$), 2 h on Day 11 (Fig. 2E, $p < 0.05$), and 2 h on Day 13 (Fig. 2F, $p < 0.05$). The anti-nociceptive

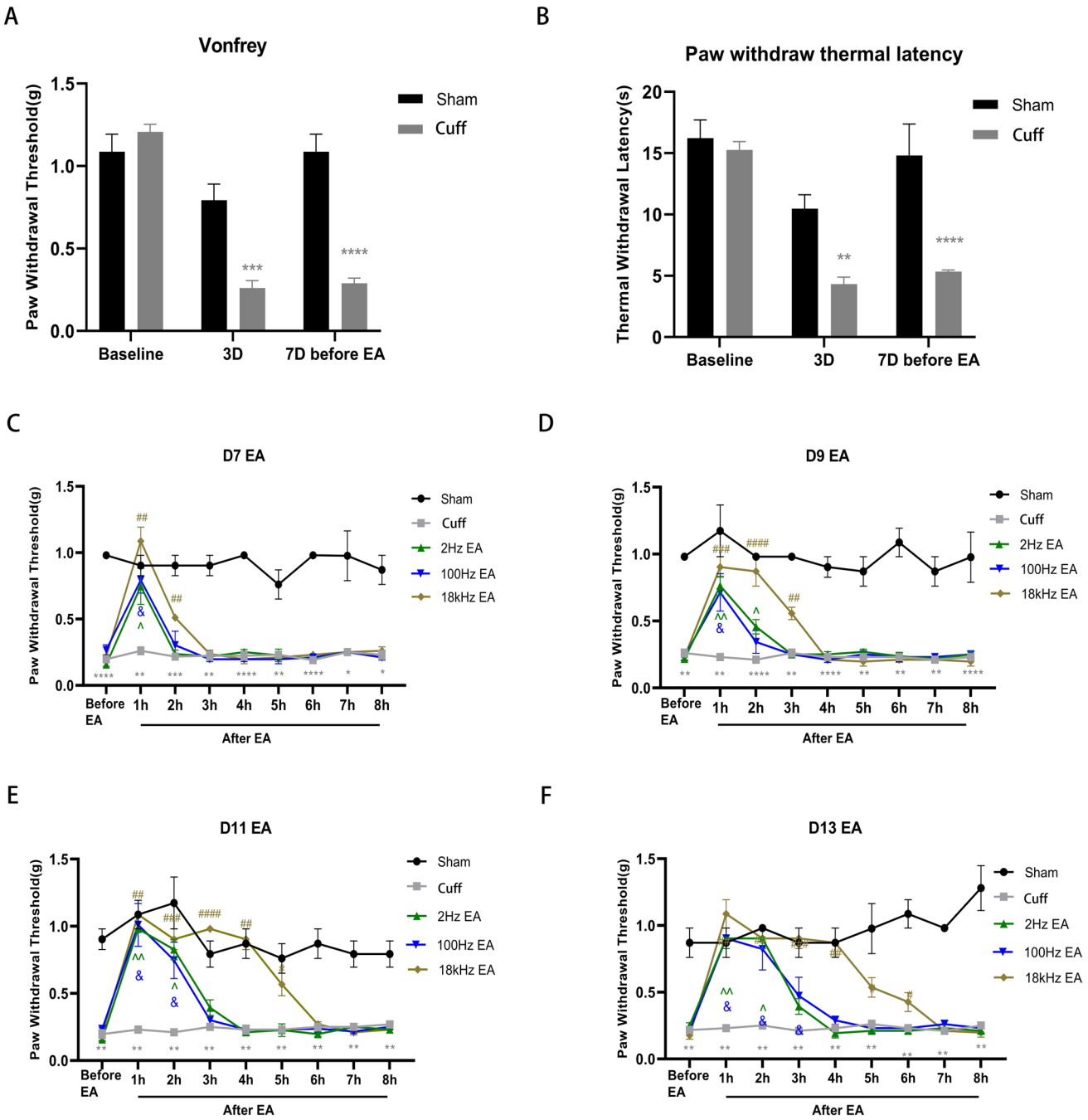

Fig. 2 Assessment of PWT and TWL before and after EA. The PWT(**A**) and TWL(**B**) of mice in the cuff group were notably lower than those in the sham group on Day 3 and Day 7 before EA. From Day 7 to Day 13, 2 Hz EA reduced mechanical pain for 1 h, followed by 2 h, another 2 h, and then 2 h. Similarly, 100 Hz EA reduced mechanical pain for 1 h, followed by 2 h, another 2 h, and then 3 h. Moreover, 18 kHz EA significantly alleviated mechanical pain for 2 h, 3 h, 5 h, and 6 h (**C-F**). All value represents the mean ($n = 10$; ± SEM). $^{*}p < 0.05$, $^{**}p < 0.01$, $^{***}p < 0.001$, $^{****}p < 0.0001$ compared to the Sham group; $^{\wedge}p < 0.05$, $^{\wedge\wedge}p < 0.01$, $\&p < 0.05$, $\#p < 0.05$, $\#\#p < 0.01$, $\#\#\#p < 0.001$, $\#\#\#\#p < 0.0001$ versus the cuff group

duration induced by 100 Hz EA was 1 h on Day 7 (Fig. 2C, $p < 0.05$), 2 h on Day 9 (Fig. 2D, $p < 0.05$), 2 h on Day 11 (Fig. 2E, $p < 0.05$), and 3 h on Day 13 (Fig. 2F, $p < 0.05$). In contrast, the anti-nociceptive duration induced by 18 kHz EA was 2 h on Day 7 (Fig. 2C, $p < 0.01$), 3 h on Day 9 (Fig. 2D, $p < 0.01$), 5 h on Day 11 (Fig. 2E, $p < 0.05$), and 6 h on Day 13 (Fig. 2F, $p < 0.05$).

The results revealed that the duration of analgesia increased in correlation with the number of days of EA. Notably, the analgesic effect achieved with 2 Hz and 100

Hz EA peaks at approximately 3 h, whereas the intervention using 18 kHz EA extends this analgesic period to 6 h. The analgesic effect of 18 kHz EA exhibited a significant enhancement with the prolongation of EA days, surpassing the effects observed with 2 Hz and 100 Hz stimulations. There was no discernible difference in analgesic effect between 2 Hz and 100 Hz stimulations.

Impact of Varying EA Frequencies on Neuropeptide Release

To elucidate the effects of diverse EA frequencies on neuropeptide secretion within the spinal cord, we conducted an in-depth analysis of endorphin, enkephalin, and dynorphin levels across multiple experimental cohorts. qRT-PCR analysis demonstrated a marked reduction in the mRNA expression of POMC, PENK, and PDYN mRNA in the cuff group relative to the sham group (Fig. 3A, $p < 0.001$ for POMC; $p < 0.01$ for

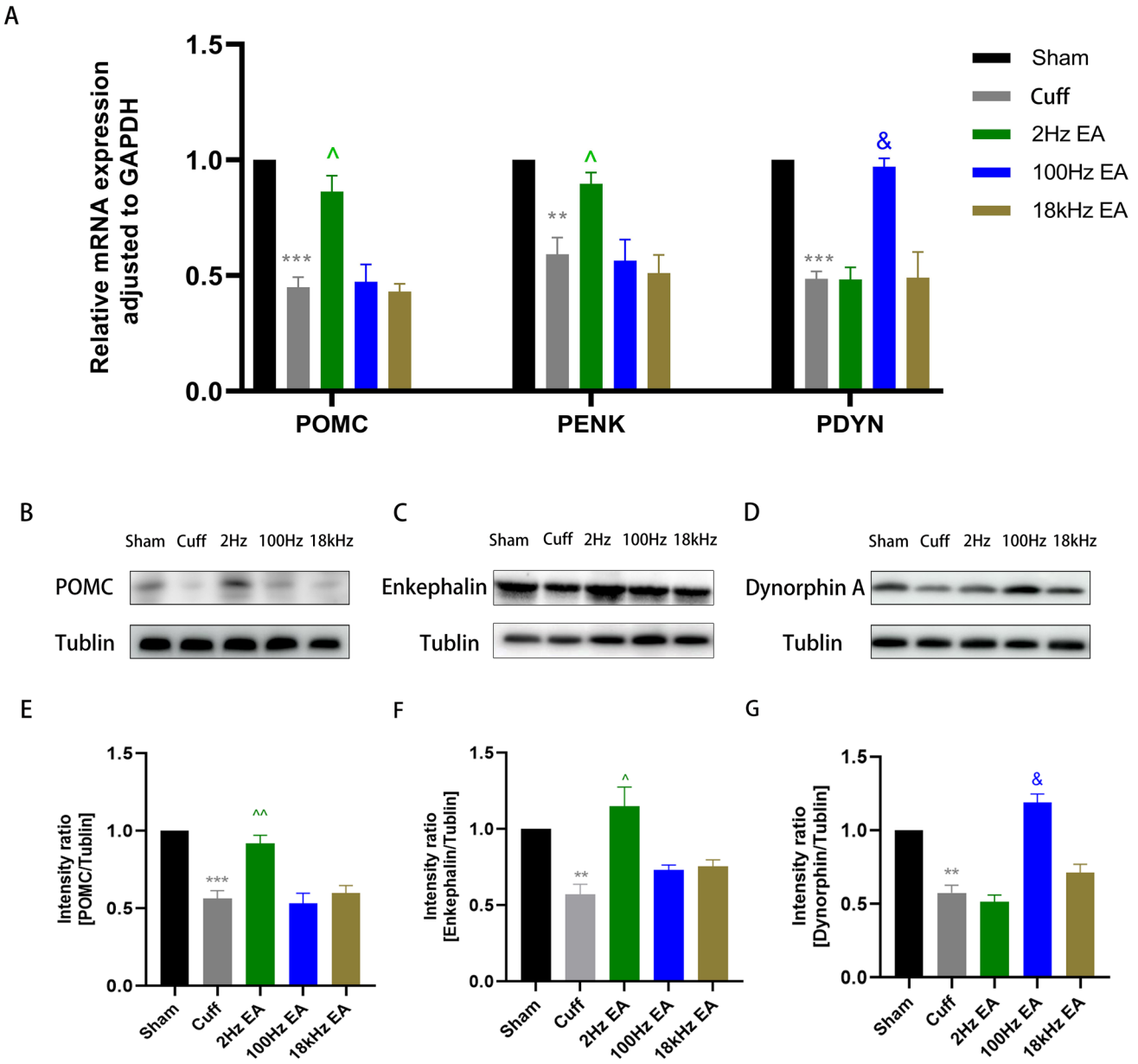

Fig. 3 The expression of neuropeptides in the spinal cord after different frequency EA. qRT-PCR was employed to evaluate the mRNA expression of POMC, PENK, and PDTN in the spinal cord. (**A**) Western blot analysis was performed to assess the protein expression levels of POMC, enkephalin and dynorphin A in the L4-L6 spinal cord. (**B-G**) All results were expressed as mean ± SEM and were statistically using one-way ANOVA followed by Tukey's post-hoc test ($n = 6$). $^{**}p < 0.01$, $^{***}p < 0.001$ compared to the Sham group; $^{\wedge}p < 0.05$, $^{\wedge\wedge}p < 0.01$, & $p < 0.05$ compared to the cuff group

PENK; $p<0.001$ for PDYN). However, treatment with 2hz EA significantly elevated POMC and PENK mRNA levels in cuff group (Fig. 3A, $p<0.05$ for POMC; $p<0.05$ for PENK), whereas 100hz EA effectively reversed the inhibitory state of PDYN mRNA (Fig. 3A, $p<0.05$ for PDYN). Notably, there were no significant changes observed in POMC, PENK, and PDYN mRNA levels in the 18 kHz EA group when compared to the cuff group (Fig. 3A). Subsequent western blotting was employed to evaluate the protein expression of these neuropeptides in the spinal cord, revealing a pronounced downregulation of POMC, enkephalin and dynorphin A in the cuff group (Fig. 3B-G, $p<0.001$ for POMC; $p<0.01$ for enkephalin; $p<0.01$ for dynorphin A). Treatment with 2 Hz EA increased the POMC and enkephalin protein levels in sciatic nerve cuffing mice (Fig. 3E-F, $p<0.01$ for POMC; $p<0.05$ for enkephalin), while 100 Hz EA effectively enhanced the expression of dynorphin A (Fig. 3G, $p<0.05$ for dynorphin A). However, the 18 kHz EA did not alter the protein levels of POMC, enkephalin and dynorphin A in the spinal cord (Fig. 3B-G). To further validate these results, we utilized immunofluorescence analysis to assess the expression and activation of POMC and dynorphin A. We observed significant inhibition of POMC and dynorphin A in the cuff group (Fig. 4A-D, $p<0.01$ for POMC; $p<0.01$ for dynorphin A). Treatment with 2 Hz EA led to a notable increase in POMC expression compared to the cuff group (Fig. 4A-B, $p<0.01$ for POMC), while 100HzEA

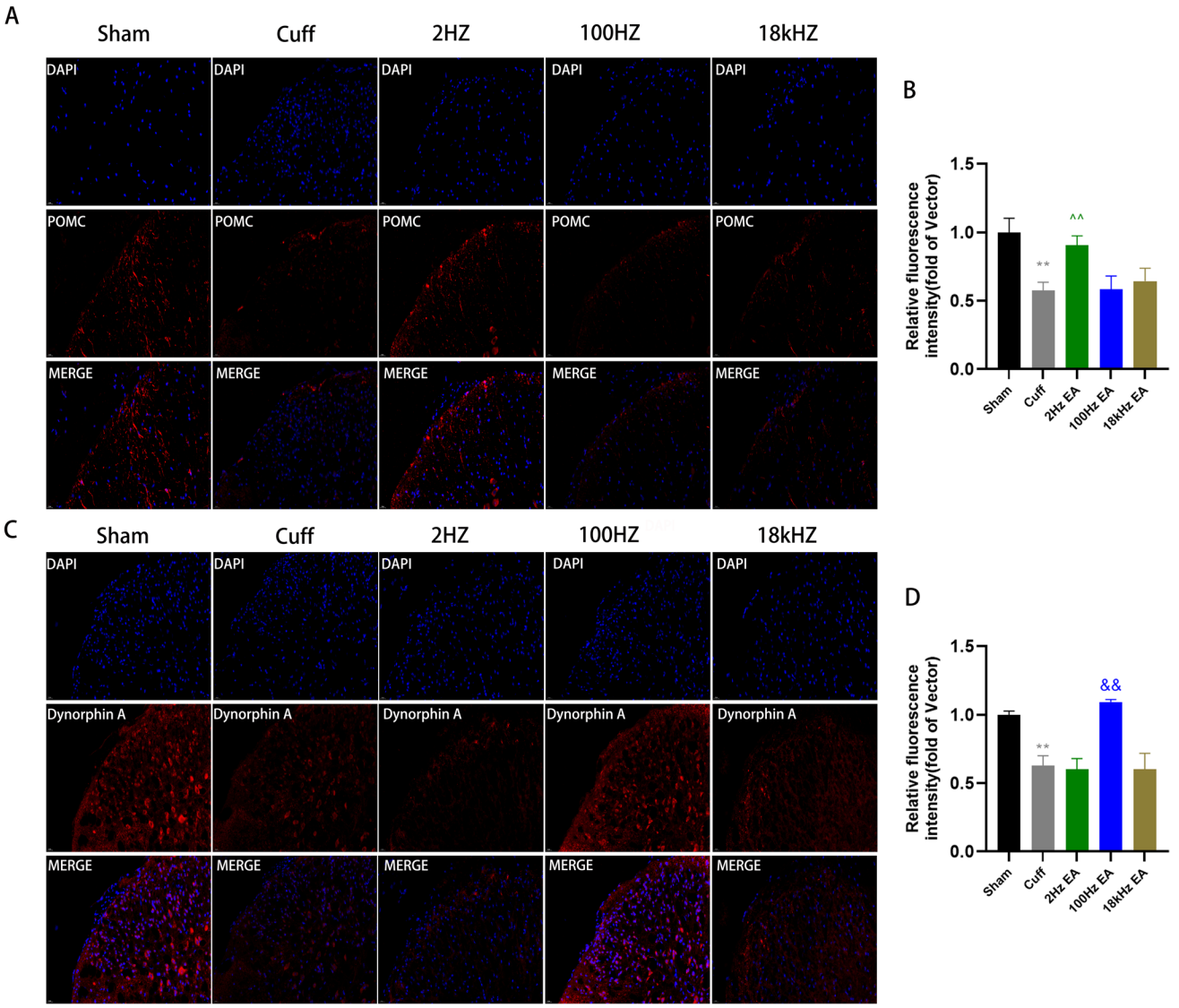

Fig. 4 The impact of EA on the expression levels of POMC and dynorphin A in the spinal cord. Immunohistochemical analyses and statistical histogram of the immunofluorescence of POMC and dynorphin A immunoreactive positive neurons with a scale bar set at 20 μm. (**A-D**) Results were presented as mean ± SEM and were analyzed using one-way ANOVA and Tukey's post-hoc test ($n=6$). Statistical significance was observed as $^{**}p<0.01$ compared to the Sham group, $^{\wedge\wedge}p<0.01$ and $\&\&p<0.01$ compared to the cuff group

resulted in increased expression of dynorphin A (Fig. 4C-D, $p < 0.01$ for dynorphin A). Notably, 18 kHz EA did not exert any influence on neuropeptide expression, thereby confirming the differential impact of varying EA frequencies on neuropeptide release within the spinal cord (Fig. 4A-D).

Influence of Varying EA Frequencies on Inflammatory Cytokines Expression

To clarify the impact of various EA frequencies on the expression of inflammatory cytokines in the spinal cord, we conducted a comprehensive analysis of IL-1β and TNF-α levels. qRT-PCR analysis revealed a significant elevation in mRNA expression of both IL-1β and TNF-α in the cuff group compared to the sham group (Fig. 5A, $p < 0.05$ for IL-1β; $p < 0.001$ for TNF-α). Treatment with 2 Hz EA, 100 Hz EA, and 18 kHz EA significantly decreased mRNA levels of IL-1β and TNF-α in the cuff group (Fig. 5A). Subsequently, western blotting was employed to assess protein expression levels of these cytokines within the spinal cord, revealing a notable upregulation of TNF-α and IL-1β in the cuff group (Fig. 5B-E, $p < 0.01$ for both IL-1β and TNF-α). Moreover, treatment with 2 Hz EA, 100 Hz EA, and 18 kHz EA effectively suppressed protein levels of IL-1β and TNF-α in sciatic nerve cuffing mice (Fig. 5B-E).

Sequencing and Assembly of Spinal Cord Tissue Data

In order to explore the mechanism of 18 kHz EA in relieving neuropathic pain, we conducted RNA-Seq on the sham group, the cuff group, and the 18 kHz EA group. Statistical analysis of three samples from each group revealed that the spinal cord tissue of the sham group yielded 149,692,394 original reads, whereas the cuff group produced 154,682,018 raw reads and the 18 kHz group generated 155,852,958 raw reads. After acquiring the data, each sample's reads were compared to a reference sequence database using Star software. Subsequently, the alignment status was statistically analyzed with RSEQC. In the sham group, 142,068,444 read segments matched the database, compared to 149,077,817 in the cuff group and 150,198,646 in the 18 kHz group. Table 2 summarized the mapping rates for each sample.

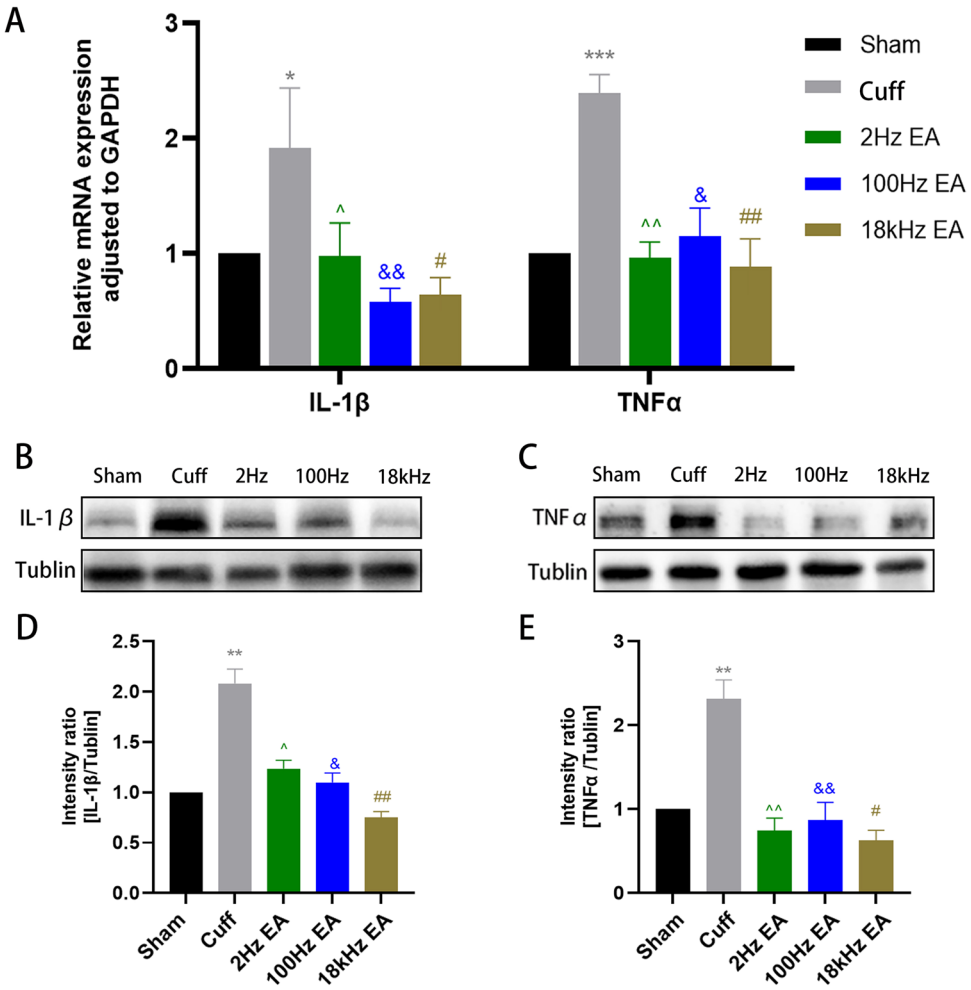

Fig. 5 The expression of inflammatory cytokines in the spinal cord after different frequency EA. qRT-PCR was employed to evaluate the mRNA expression of IL-1β and TNF-α in the spinal cord. (**A**) Western blot analysis was performed to assess the protein expression levels of IL-1β and TNF-α in the L4-L6 spinal cord. (**B-E**) All results were expressed as mean ± SEM and were statistically using one-way ANOVA followed by Tukey's post-hoc test ($n = 6$). *$p < 0.05$, **$p < 0.01$, ***$p < 0.001$ compared to the Sham group; ^$p < 0.05$, ^^$p < 0.01$, & $p < 0.05$, && $p < 0.01$, #$p < 0.05$, ## $p < 0.01$ compared to the cuff group

Table 2 The reads mapping rate of each sample in those three groups

Sample	Total clean reads	Total mapped	Mapped ratio (%)
Sham1	48,593,808	44,924,745	92.40%
Sham2	48,170,536	46,263,782	96.00%
Sham3	52,928,050	50,879,917	96.10%
Cuff1	51,114,420	49,347,408	96.50%
Cuff2	49,426,744	47,501,526	96.10%
Cuff3	54,140,854	52,228,883	96.50%
18kHz1	45,220,200	43,555,210	96.30%
18kHz2	48,944,732	47,187,311	96.40%
18kHz3	61,688,026	59,456,125	96.40%

Analysis of the Differentially Expressed Genes (Cuff vs. 18 kHz EA)

We employed the DESeq2 software to analyze differential gene expression between the Cuff and 18 kHz EA groups, resulting in the detection of a total of 476 genes exhibiting varied expression patterns. In constructing the volcano plot, each data point represented an individual gene, with log2FC values depicted on the x-axis. We defined $|\log2FC| \geq 1$ as the threshold for significant differences in gene expression and observed that compared to the cuff group, there were 216 significantly upregulated genes (≥ 1) in the 18 kHz EA group, along with 260 significantly downregulated genes ($\leq$-1). The y-axis represented -log10(P-Value), where genes were considered significantly different when P-Value was ≤ 0.05 (Fig. 6A). Additionally, we performed bidirectional hierarchical clustering on differentially expressed genes across samples and visualized these results using a heatmap (Fig. 6B).

Investigation of Differential Gene Ontology Functions and KEGG Pathway Enrichment

GO encompasses molecular function (MF), biological process (BP), and cellular component (CC). In comparison to the cuff group, the 18 kHz group exhibited differential expression of 347 genes in the BP group, 36 genes in the CC group, and 84 genes in the MF group. GO enrichment analysis was conducted on the differentially expressed genes from both groups. The results revealed that 18 kHz EA influenced various biological processes such as cellular responses to cytokine stimulation and calcium-mediated signal transduction utilizing intracellular calcium sources. Additionally, it impacted cellular components including cluster of actin-based cell projections and muscle myosin complex, as well as molecular functions like neurotransmitter receptor activity (Fig. 7A). Furthermore, pathway enrichment analysis using the KEGG database indicated that differential gene expression in the 18 kHz group was predominantly enriched in pathways related to serotonergic synapses, G protein-gated Potassium channels, Inflammatory mediator regulation of TRP channels, TNF signaling pathway, voltage-gated Ca2+channels via G beta/gamma subunits, and cell adhesion molecules (CAMs)

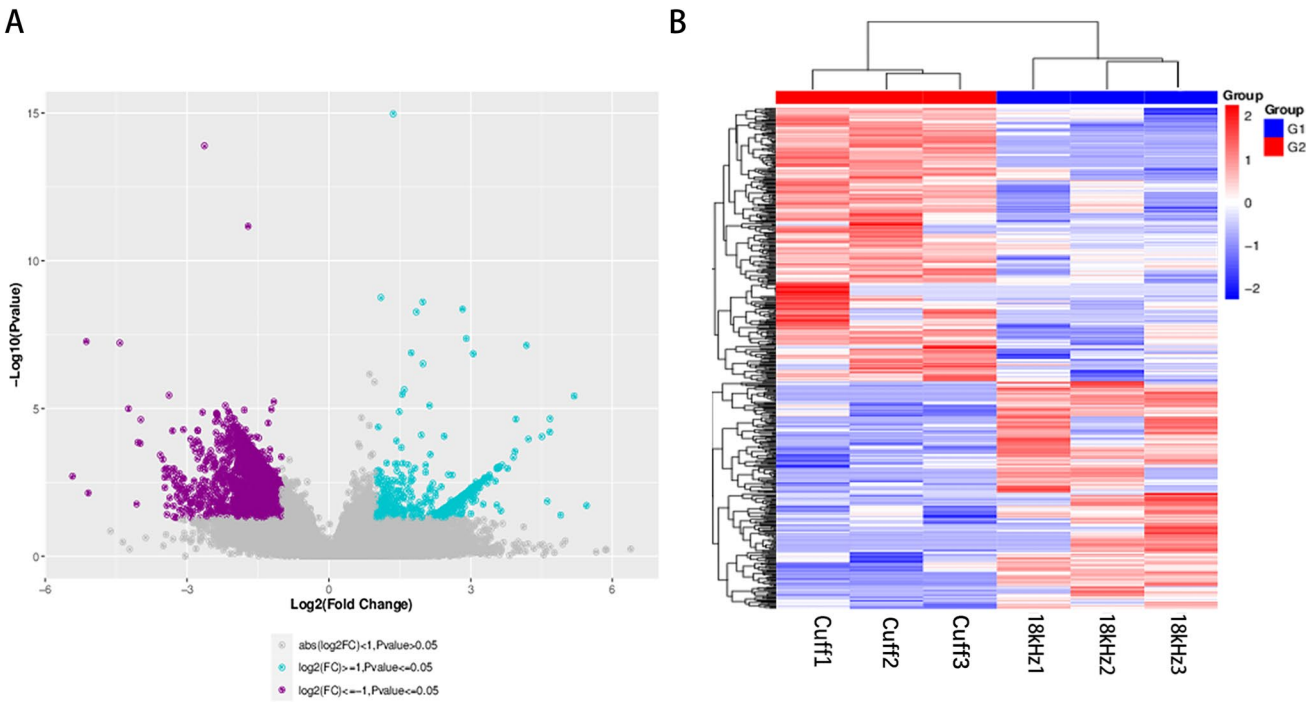

Fig. 6 The upregulated and downregulated genes. Setting $p < 0.05$ and $|\log2FC| \geq 1.0$ as cutoff values

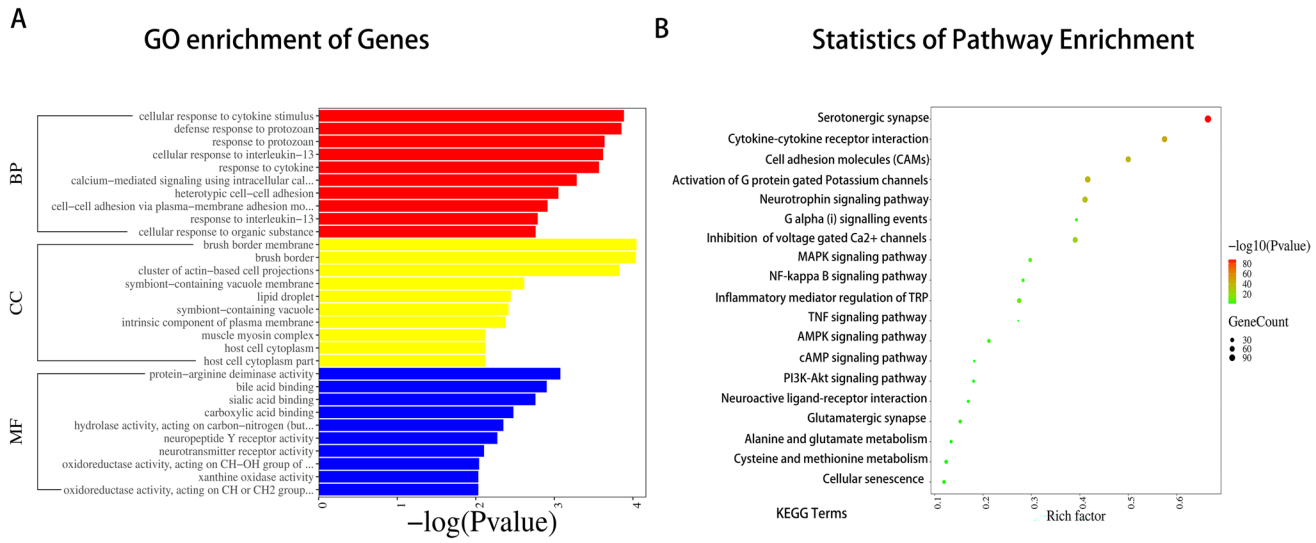

Fig. 7 Gene enrichment analysis of the spinal cord concerning Cellular Component (CC), Biological Process (BP) and Molecular Function (MF) in the 18 kHz group as compared with the cuff group. (**A**) Enriched pathways from KEGG analysis of differentially expressed genes between the cuff group and 18 kHz group. (**B**)

pathways (Fig. 7B). The evidence indicated the potential involvement of the serotonin system in mediating the analgesic effects of KHES, and our sequencing findings also spurred further investigation into the role of endogenous spinal 5-HT in KHES within animal models.

18 kHz EA Relieving Neuropathic Pain Via the 5-HT Pathway

The qRT-PCR findings indicated a notable decrease in the mRNA levels of 5-HT1A, 5-HT1B, 5-HT3A, 5-HT4A, and 5-HT5A in cuff group (Fig. 8A, $p<0.01$ for 5-HT1A and 5-HT1B; $p<0.05$ for 5-HT3A, 5-HT4A, and 5-HT5A), accompanied by markedly reduced mRNA levels of GIRK1, GIRK2

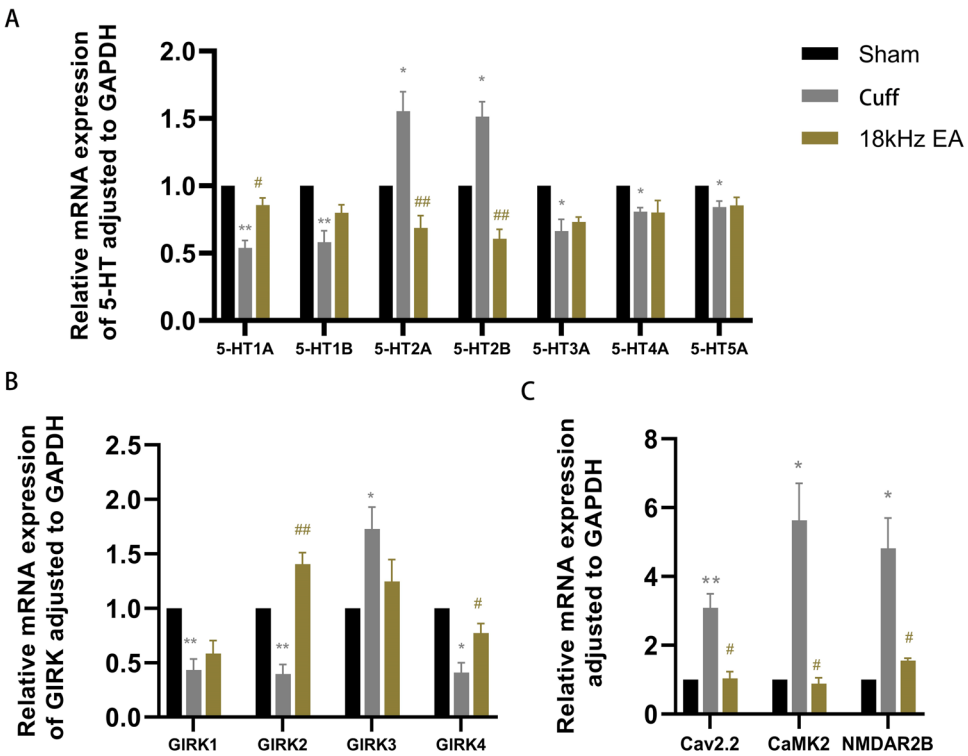

Fig. 8 The mRNA levels of some related genes in the spinal cord detected by qRT-PCR. All the results were expressed as mean ± SEM and analyzed by one-way ANOVA followed by Tukey's post hoc tests ($n=6$). * $p<0.05$, ** $p<0.01$ versus the Sham group; # $p<0.05$, ## $p<0.01$ versus the cuff group

and GIRK4 (Fig. 8B, $p<0.01$ for GIRK1 and GIRK2; $p<0.05$ for GIRK4). Additionally, there was a significant rise in the mRNA levels of 5-HT2A and 5-HT2B in cuff group (Fig. 8A, $p<0.05$ for 5-HT2A and 5-HT2B), accompanied by markedly increased mRNA levels of GIRK3, Cav2.2, CaMKII, and NMDAR2B (Fig. 8B, $p<0.05$ for GIRK3; Fig. 8C, $p<0.01$ for Cav2.2; $p<0.05$ for CaMKII and NMDAR2B). After 18 kHz EA, the mRNA levels of 5-HT1A, GIRK2 and GIRK4 were significantly increased in cuff mice (Fig. 8A, $p<0.05$ for 5-HT1A; Fig. 8B, $p<0.01$ for GIRK2; $p<0.05$ for GIRK4), while the levels of 5-HT2A, 5-HT2B, Cav2.2, CaMKII, and NMDAR2B were significantly decreased (Fig. 8A, $p<0.01$ for 5-HT2A and 5-HT2B; Fig. 8C, $p<0.05$ for Cav2.2, CaMKII and NMDAR2B).

Discussion

In this study involving commonly used frequencies—2 Hz, 100 Hz, and 18 kHz—all frequencies significantly reduced hyperalgesia in sciatic nerve cuffing mice following neural trauma, with the 18 kHz EA showing a more persistent analgesic effect. Although clear evidence has been presented on the analgesic effects of different frequencies, further comprehensive research is necessary to elucidate the potential differences in their mechanisms of action (Xiang et al. 2014). Previous studies have shown that endogenous opioid peptides coexist with other neuropeptides or neurotransmitters in both the central and peripheral nervous systems, creating a robust intrinsic pain modulation system that governs pain regulation. EA achieves its analgesic effects by enhancing the release of endogenous opioids and modulating the associated receptors. Professor Han Jisheng's research team has been investigating how EA influences centrally-mediated analgesia. They believe that 2 Hz stimulation promotes the release of endorphin and enkephalin, which targets μ-δ receptors, while 100 Hz stimulation increases the discharge of potent opioids, activating K-receptors. Alternating between these two frequencies results in the simultaneous release of four opioid peptides (Han 2004). These peptides activate downstream opioid receptors through G-protein coupling, leading to the liberation of neurotransmitters including norepinephrine, acetylcholine, dopamine, and substance P from nerve endings. This process hyperpolarizes the postsynaptic membranes, impedes the transmission of nociceptive impulses, and thereby produces analgesia (Han 2003). The endocrine hormones and neurotransmitters released by electrical stimulation do not dissipate immediately upon cessation of the stimulation; instead, they continue to exert their influence within the body. It is crucial to emphasize that acupuncture analgesia is a highly intricate process involving multiple levels, channels, and targets, both peripheral and central (Du et al. 2020), as well as the opioid peptide system (Dembla et al. 2017), cannabinoid system (Yuan et al. 2018), purinergic signaling (Liao et al. 2017), and numerous other aspects including inflammatory cytokines (Zhao 2008). Based on this foundation, this article focused on the direction of neuropeptides and inflammatory factors secretion to compare differences in analgesic mechanisms at different frequencies with the aim of delving more deeply into the secrets of acupuncture analgesia. Our study demonstrated that frequencies of 2 Hz, 100 Hz, and 18 kHz effectively attenuate the release of inflammatory cytokines in the spinal cord of mice with neuropathic pain, however, distinct frequencies exert varying effects on neuropeptide release within the spinal cord. We revealed that frequencies of 2 Hz and 100 Hz can effectively modulate spinal neuropeptide secretion, resulting in relief from neuropathic pain; however, the frequency of 18 kHz had no discernible effect on neuropeptide levels. Given the current scarcity of research on the analgesic mechanisms of KHES and its unclear mode of action, subsequent studies were exclusively dedicated to mechanism screening for 18 kHz EA, with only RNA-seq and qRT-PCR conducted on the 18 kHz EA group. The results indicated that 18 kHz may alleviate hyperalgesia in sciatic nerve cuffing mice by modulating the 5-HT pathway (Supplementary Fig. 1).

5-HT is primarily synthesized by serotonergic neurons located in the raphe nuclei of the brain. It is then transported downwards through projection fibers to the dorsal horn of the spinal cord, where it manifests its effects by binding to its respective receptors (Kaswan et al. 2021; Newman-Tancredi et al. 2018; Okaty et al. 2019). The 5-HT receptor family comprises seven distinct subfamilies and fifteen subtypes, which are instrumental in regulating pain, mood, and sleep (Albert and Vahid-Ansari 2019; Artola et al. 2020; Pineda-Farias et al. 2015). Moreover, they are integral to the regulatory mechanisms governing neuropathic pain and central sensitization. Our study revealed significant variations in the expression levels of 5-HT receptors, Cav2.2 N-type calcium channels, GIRK2 inward rectifier potassium channels, NMDA receptors, and their downstream CaMKII molecules using RNA-seq and qRT-PCR before and after KHES stimulation. Drawing from these findings, we advance the following scientific hypothesis: KHES has the potential to augment the axonal projection of 5-HT neurons subsequent to nerve injury, thereby enhancing the release of 5-HT. Spinal cord neurons increase the expression of 5-HT1 receptors, leading to a reduction in the openness of the Cav2.2 channel and a decrease in calcium ion influx, thus dampening the excitability of spinal cord neurons and mitigating long-term potentiation (LTP). Concurrently, the downregulation of 5-HT2 receptors curbs the activity of spinal glial cells, diminishing the release of neuroactive substances, and ultimately alleviating chronic neuropathic pain.

Our study has several notable limitations. We primarily focus on commonly used frequencies such as 2 Hz, 100 Hz, and 18

kHz, which play a representative role in this investigation. However, future studies should explore the application of EA at additional frequencies and for various types of pain. When comparing the analgesic effects of the three frequency groups, our assessment is confined to differences within a 7-day period. To gain a better understanding of potential long-term analgesic disparities between different frequencies of EA, it is necessary to enhance our evaluation of long-term effects and extend the experimental duration. Moving forward, our future research will delve deeper into the mechanisms by which KHES alleviates neuropathic pain. Specifically, we will focus on the impact of various subtypes of 5-HT receptors as target proteins on neuronal synaptic plasticity and downstream neuroglia cell in the spinal cord.

Conclusions

Our results demonstrated that the analgesic effect of EA on neuropathic pain in mice was frequency-dependent. Stimulation at 18 kHz provided superior and prolonged relief compared to 2 Hz and 100 Hz. Frequencies of 2 Hz, 100 Hz, and 18 kHz significantly reduced the release of inflammatory cytokines (IL-1β and TNF-α) in the spinal cord of mice suffering from neuropathic pain. While 2 Hz EA enhanced the release of endorphins and enkephalin, and 100 Hz EA increased the secretion of dynorphin, 18 kHz EA did not affect spinal neuropeptide levels. Furthermore, 18 kHz stimulation reduced spinal neuronal excitability by modulating the serotonergic pathway and downstream receptors in the spinal cord to alleviate neuropathic pain.

Supplementary Information The online version contains supplementary material available at https://doi.org/10.1007/s12031-024-02276-6.

Author Contributions BY and KXF concepted and designed this study. KXF and WC performed the research and analyzed the results. KXF wrote the manuscript and prepared the figures and tables. All authors reviewed the manuscript.

Funding This work was supported by Shanghai Rehabilitation Medical Research Center [grant numbers 2023ZZ02027] and National Natural Science Foundation of China [grant numbers 82471242].

Data Availability No datasets were generated or analysed during the current study.

Declarations

Competing Interests The authors declare no competing interests.

References

Albert PR, Vahid-Ansari F (2019) The 5-HT1A receptor: signaling to behavior. Biochimie 161:34–45. https://doi.org/10.1016/j.biochi.2018.10.015

Artola A, Voisin D, Dallel R (2020) PKCγ interneurons, a gateway to pathological pain in the dorsal horn. J Neural Transm (Vienna) 127(4):527–540. https://doi.org/10.1007/s00702-020-02162-6

Attal N, Cruccu G, Baron R, Haanpää M, Hansson P, Jensen TS et al (2010) EFNS guidelines on the pharmacological treatment of neuropathic pain: 2010 revision. Eur J Neurol 17(9):1113-e1188. https://doi.org/10.1111/j.1468-1331.2010.02999.x

Benbouzid M, Pallage V, Rajalu M, Waltisperger E, Doridot S, Poisbeau P et al (2008) Sciatic nerve cuffing in mice: a model of sustained neuropathic pain. Eur J Pain 12(5):591–599. https://doi.org/10.1016/j.ejpain.2007.10.002

Chaplan SR, Bach FW, Pogrel JW, Chung JM, Yaksh TL (1994) Quantitative assessment of tactile allodynia in the rat paw. J Neurosci Methods 53(1):55–63. https://doi.org/10.1016/0165-0270(94)90144-9

Chen XH, Han JS (1992) Analgesia induced by electroacupuncture of different frequencies is mediated by different types of opioid receptors: another cross-tolerance study. Behav Brain Res 47(2):143–149. https://doi.org/10.1016/s0166-4328(05)80120-2

Chen T, Taniguchi W, Chen QY, Tozaki-Saitoh H, Song Q, Liu RH et al (2018) Top-down descending facilitation of spinal sensory excitatory transmission from the anterior cingulate cortex. Nat Commun 9(1):1886. https://doi.org/10.1038/s41467-018-04309-2

Chen XM, Xu J, Song JG, Zheng BJ, Wang XR (2015) Electroacupuncture inhibits excessive interferon-γ evoked up-regulation of P2×4 receptor in spinal microglia in a CCI rat model for neuropathic pain. Br J Anaesth 114(1):150–157. https://doi.org/10.1093/bja/aeu199

Cortes-Altamirano JL, Olmos-Hernandez A, Jaime HB, Carrillo-Mora P, Bandala C, Reyes-Long S et al (2018) Review: 5-HT1, 5-HT2, 5-HT3 and 5-HT7 receptors and their role in the modulation of pain response in the central nervous System. Curr Neuropharmacol 16(2):210–221. https://doi.org/10.2174/1570159x15666170911121027

Cuitavi J, Hipólito L, Canals M (2021) The life cycle of the Mu-Opioid receptor. Trends Biochem Sci 46(4):315–328. https://doi.org/10.1016/j.tibs.2020.10.002

Dembla S, Behrendt M, Mohr F, Goecke C, Sondermann J, Schneider FM et al (2017) Anti-nociceptive action of peripheral mu-opioid receptors by G-beta-gamma protein-mediated inhibition of TRPM3 channels. Elife 6:e26280. https://doi.org/10.7554/eLife.26280

Du J, Fang J, Xu Z et al (2020) Electroacupuncture suppresses the pain and pain-related anxiety of chronic inflammation in rats by increasing the expression of the NPS/NPSR system in the ACC. Brain Res 1733:146719. https://doi.org/10.1016/j.brainres.2020.146719

Dworkin RH, O'Connor AB, Kent J, Mackey SC, Raja SN, Stacey BR et al (2013) Interventional management of neuropathic pain: NeuPSIG recommendations. Pain 154(11):2249–2261. https://doi.org/10.1016/j.pain.2013.06.004

Fan Z, Dou B, Wang J et al (2023) Effects and mechanisms of acupuncture analgesia mediated by afferent nerves in acupoint microenvironments. Front Neurosci 17:1239839. https://doi.org/10.3389/fnins.2023.1239839

Fang K, Lu P, Cheng W, Yu B (2024) Kilohertz high-frequency electrical stimulation ameliorate hyperalgesia by modulating transient receptor potential vanilloid-1 and N-methyl-D-aspartate receptor-2B signaling pathways in chronic constriction injury of sciatic nerve mice. Mol Pain 20:17448069231225810. https://doi.org/10.1177/17448069231225810

Gilron I, Baron R, Jensen T (2015) Neuropathic pain: principles of diagnosis and treatment. Mayo Clin Proc 90(4):532–545. https://doi.org/10.1016/j.mayocp.2015.01.018

Haleem DJ (2018) Serotonin-1A receptor dependent modulation of pain and reward for improving therapy of chronic pain. Pharmacol Res 134:212–219. https://doi.org/10.1016/j.phrs.2018.06.030

Han JS (2003) Acupuncture: neuropeptide release produced by electrical stimulation of different frequencies. Trends Neurosci 26(1):17–22. https://doi.org/10.1016/s0166-2236(02)00006-1

Han JS (2004) Acupuncture and endorphins. Neurosci Lett 361(1–3):258–261. https://doi.org/10.1016/j.neulet.2003.12.019

Hargreaves K, Dubner R, Brown F, Flores C, Joris J (1988) A new and sensitive method for measuring thermal nociception in cutaneous hyperalgesia. Pain 32(1):77–88. https://doi.org/10.1016/0304-3959(88)90026-7

Heijmans L, Mons MR, Joosten EA (2021) A systematic review on descending serotonergic projections and modulation of spinal nociception in chronic neuropathic pain and after spinal cord stimulation. Mol Pain 17:17448069211043965. https://doi.org/10.1177/17448069211043965

Jiang B, Zhong X, Fang J, Zhang A, Wang DW, Liang Y et al (2021) Electroacupuncture attenuates Morphine Tolerance in rats with Bone Cancer Pain by inhibiting PI3K/Akt/JNK1/2 signaling pathway in the spinal dorsal horn. Integr Cancer Ther 20:1534735421995237. https://doi.org/10.1177/1534735421995237

Jiang Z, Li Y, Wang Q et al (2022) Combined-acupoint electroacupuncture induces better analgesia via activating the endocannabinoid system in the spinal cord. Neural Plast 2022:7670629. https://doi.org/10.1155/2022/7670629

Kaswan NK, Mohammed Izham NAB, Tengku Mohamad TAS, Sulaiman MR, Perimal EK (2021) Cardamonin modulates neuropathic pain through the possible involvement of serotonergic 5-HT1A receptor pathway in CCI-induced neuropathic pain mice model. Molecules 26(12):3677. https://doi.org/10.3390/molecules26123677

Knotkova H, Hamani C, Sivanesan E, Le Beuffe MFE, Moon JY, Cohen SP et al (2021) Neuromodulation for chronic pain. Lancet 397(10289):2111–2124. https://doi.org/10.1016/s0140-6736(21)00794-7

Lee HG, Kim WM, Kim JM, Bae HB, Choi JI (2015) Intrathecal nefopam-induced antinociception through activation of descending serotonergic projections involving spinal 5-HT7 but not 5-HT3 receptors. Neurosci Lett 587:120–125. https://doi.org/10.1016/j.neulet.2014.12.040

Lee HJ, Lee JH, Lee EO, Lee HJ, Kim KH, Lee KS et al (2009) Substance P and beta endorphin mediate electroacupuncture induced analgesic activity in mouse cancer pain model. Acupunct Electrother Res 34(1–2):27–40. https://doi.org/10.3727/036012909803861095

Li Y, Fang Z, Gu N, Bai F, Ma Y, Dong H et al (2019) Inhibition of chemokine CX3CL1 in spinal cord mediates the electroacupuncture-induced suppression of inflammatory pain. J Pain Res 12:2663–2672. https://doi.org/10.2147/jpr.S205987

Liao HY, Hsieh CL, Huang CP, Lin YW (2017) Electroacupuncture attenuates CFA-induced Inflammatory Pain by suppressing Nav1.8 through S100B, TRPV1, opioid, and Adenosine pathways in mice. Sci Rep 7:42531. https://doi.org/10.1038/srep42531

Ling D, Luo J, Wang M, Cao X, Chen X, Fang K et al (2019) Kilohertz high-frequency alternating current blocks nerve conduction without causing nerve damage in rats. Ann Transl Med 7(22):661. https://doi.org/10.21037/atm.2019.10.36

Lu P, Fang K, Cheng W, Yu B (2023) High-frequency electrical stimulation reduced hyperalgesia and the activation of the Myd88 and NFκB pathways in chronic constriction injury of sciatic nerve-induced neuropathic pain mice. Neurosci Lett 796:137064. https://doi.org/10.1016/j.neulet.2023.137064

Miller JP, Eldabe S, Buchser E, Johanek LM, Guan Y, Linderoth B (2016) Parameters of spinal cord stimulation and their role in Electrical Charge Delivery: a review. Neuromodulation 19(4):373–384. https://doi.org/10.1111/ner.12438

Mo SY, Xue Y, Li Y, Zhang YJ, Xu XX, Fu KY et al (2023) Descending serotonergic modulation from rostral ventromedial medulla to spinal trigeminal nucleus is involved in experimental occlusal interference-induced chronic orofacial hyperalgesia. J Headache Pain 24(1):50. https://doi.org/10.1186/s10194-023-01584-3

Mosconi T, Kruger L (1996) Fixed-diameter polyethylene cuffs applied to the rat sciatic nerve induce a painful neuropathy: ultrastructural morphometric analysis of axonal alterations. Pain 64(1):37–57. https://doi.org/10.1016/0304-3959(95)00077-1

Newman-Tancredi A, Bardin L, Auclair A, Colpaert F, Depoortère R, Varney MA (2018) NLX-112, a highly selective 5-HT(1A) receptor agonist, mediates analgesia and antidepressant-like activity in rats via spinal cord and prefrontal cortex 5-HT(1A) receptors, respectively. Brain Res 1688:1–7. https://doi.org/10.1016/j.brainres.2018.03.016

Oberoi D, Reed EN, Piedalue KA, Landmann J, Carlson LE (2022) Exploring patient experiences and acceptability of group vs. individual acupuncture for Cancer-related pain: a qualitative study. BMC Complement Med Ther 22(1):155. https://doi.org/10.1186/s12906-022-03600-6

Okaty BW, Commons KG, Dymecki SM (2019) Embracing diversity in the 5-HT neuronal system. Nat Rev Neurosci 20(7):397–424. https://doi.org/10.1038/s41583-019-0151-3

Pineda-Farias JB, Velázquez-Lagunas I, Barragán-Iglesias P, Cervantes-Durán C, Granados-Soto V (2015) 5-HT(2B) receptor antagonists reduce nerve Injury-Induced Tactile Allodynia and expression of 5-HT(2B) receptors. Drug Dev Res 76(1):31–39. https://doi.org/10.1002/ddr.21238

Pitcher GM, Ritchie J, Henry JL (1999) Nerve constriction in the rat: model of neuropathic, surgical and central pain. Pain 83(1):37–46. https://doi.org/10.1016/s0304-3959(99)00085-8

Sánchez-Brualla I, Boulenguez P, Brocard C, Liabeuf S, Viallat-Lieutaud A, Navarro X et al (2018) Activation of 5-HT(2A) receptors restores KCC2 function and reduces neuropathic pain after spinal cord injury. Neuroscience 387:48–57. https://doi.org/10.1016/j.neuroscience.2017.08.033

Schwaller F, Kanellopoulos AH, Fitzgerald M (2017) The developmental emergence of differential brainstem serotonergic control of the sensory spinal cord. Sci Rep 7(1):2215. https://doi.org/10.1038/s41598-017-02509-2

Soin A, Shah NS, Fang ZP (2015) High-frequency electrical nerve block for postamputation pain: a pilot study. Neuromodulation 18(3):197–205. https://doi.org/10.1111/ner.12266

Tavares I, Lima D (2002) The caudal ventrolateral medulla as an important inhibitory modulator of pain transmission in the spinal cord. J Pain 3(5):337–346. https://doi.org/10.1054/jpai.2002.127775

Thuvarakan K, Zimmermann H, Mikkelsen MK, Gazerani P (2020) Transcutaneous Electrical nerve Stimulation as A Pain-Relieving Approach in Labor Pain: a systematic review and Meta-analysis of

Randomized controlled trials. Neuromodulation 23(6):732–746. https://doi.org/10.1111/ner.13221

Tiede J, Brown L, Gekht G, Vallejo R, Yearwood T, Morgan D (2013) Novel spinal cord stimulation parameters in patients with predominant back pain. Neuromodulation 16(4):370–375. https://doi.org/10.1111/ner.12032

Varga BR, Streicher JM, Majumdar S (2023) Strategies towards safer opioid analgesics-A review of old and upcoming targets. Br J Pharmacol 180(7):975–993. https://doi.org/10.1111/bph.15760

Wang Q, Mao L, Han J (1990) Analgesic electrical stimulation of the hypothalamic arcuate nucleus: tolerance and its cross-tolerance to 2 hz or 100 hz electroacupuncture. Brain Res 518(1–2):40–46. https://doi.org/10.1016/0006-8993(90)90951-7

Wu LZ, Cui CL, Tian JB, Ji D, Han JS (1999) Suppression of morphine withdrawal by electroacupuncture in rats: dynorphin and kappa-opioid receptor implicated. Brain Res 851(1–2):290–296. https://doi.org/10.1016/s0006-8993(99)02069-7

Xiang XH, Chen YM, Zhang JM, Tian JH, Han JS, Cui CL (2014) Low- and high-frequency transcutaneous electrical acupoint stimulation induces different effects on cerebral μ-opioid receptor availability in rhesus monkeys. J Neurosci Res 92(5):555–563. https://doi.org/10.1002/jnr.23351

Xu WD, Zhu B, Rong PJ, Bei H, Gao XY, Li YQ (2003) The pain-relieving effects induced by electroacupuncture with different intensities at homotopic and heterotopic acupoints in humans. Am J Chin Med 31(5):791–802. https://doi.org/10.1142/s0192415x03001478

Yu ML, Wei RD, Zhang T, Wang JM, Cheng Y, Qin FF et al (2020) Electroacupuncture relieves Pain and attenuates inflammation progression through inducing IL-10 production in CFA-Induced mice. Inflamm 43(4):1233–1245. https://doi.org/10.1007/s10753-020-01203-2

Yuan XC, Wang Q, Su W, Li HP, Wu CH, Gao F et al (2018) Electroacupuncture potentiates peripheral CB2 receptor-inhibited chronic pain in a mouse model of knee osteoarthritis. J Pain Res 11:2797–2808. https://doi.org/10.2147/jpr.S171664

Zhao ZQ (2008) Neural mechanism underlying acupuncture analgesia. Prog Neurobiol 85(4):355–375. https://doi.org/10.1016/j.pneurobio.2008.05.004

Zhou L, Stahl EL, Lovell KM, Frankowski KJ, Prisinzano TE, Aubé J et al (2015) Characterization of kappa opioid receptor mediated, dynorphin-stimulated [35S]GTPγS binding in mouse striatum for the evaluation of selective KOR ligands in an endogenous setting. Neuropharmacol 99:131–141. https://doi.org/10.1016/j.neuropharm.2015.07.001